

Article

Efficient Reduction of Bromate by Iodide-Assisted UV/Sulfite Process

Tuoqiao Zhang ¹, Jiajie Wang ¹, Dingyun Yan ², Lili Wang ³ and Xiaowei Liu ^{1,2,*}

¹ Institute of Municipal Engineering, College of Civil Engineering and Architecture, Zhejiang University, Hangzhou 310058, China; ztq@zju.edu.cn (T.Z.); wangjiajiechn@zju.edu.cn (J.W.)

² Institute of Water Resources & Ocean Engineering, Ocean College, Zhejiang University, Hangzhou 310058, China; yandingyun@zju.edu.cn

³ Environmental Engineering, Jiyang College of Zhejiang A & F University, Zhuji 311800, China; liilive@163.com

* Correspondence: liuxiaowei@zju.edu.cn; Tel.: +86-571-8820-8721

Received: 7 November 2018; Accepted: 8 December 2018; Published: 11 December 2018



Abstract: Bromate (BrO_3^-) residue in drinking water poses a great health risk. Ultra-fast reduction of BrO_3^- , under aerobic conditions, was realized using an ultraviolet (UV)/sulfite process in the presence of iodide (UV/sulfite/iodide). The UV/sulfite/iodide process produced BrO_3^- removal efficiency of 100% at about 5 min with complete conversion to bromide, while UV/sulfite induced 13.1% BrO_3^- reduction under the same conditions. Hydrated electrons, generated from the photolysis of sulfite and iodide, was confirmed as the main contributor to BrO_3^- degradation (77.4% of the total contribution). As the concentration of iodide was kept constant, its presence remarkably enhancing the generation of hydrated electrons led to its consideration as a homogeneous catalyst in the UV/sulfite/iodide system. Sulfite played a role not only as a hydrated electron precursor, but also as a reactive iodine species shielding agent and a regenerant of iodide. Results surrounding the effects on common water quality parameters (pH, bicarbonate, nitrate, natural organic matter, and solution temperature) indicated that preferred degradation of BrO_3^- occurred in an environment of alkaline pH, low-content natural organic matter/bicarbonate/nitrate, and high natural temperature.

Keywords: bromate; sulfite; iodide; photoreduction

1. Introduction

Bromate (BrO_3^-) is considered as a carcinogen, and is produced during bromide-containing water treatment processes including chlorination, ozonation, and advanced oxidation [1]. It is of great importance to remove the formed BrO_3^- in drinking water due to its carcinogenic risk. Notably, once BrO_3^- is generated in the disinfection unit of a drinking water plant, there are limited steps to prevent the occurrence of BrO_3^- in tap water. One solution is to install household water purifiers to remove BrO_3^- . The small site occupancy for household water purifiers means that the technologies adopted must remove BrO_3^- within a short contact time and at high operational cost. The methods of degrading BrO_3^- from drinking water include activated carbon or resin adsorption [2], electron beam irradiation [3], membrane separation [4], biological reduction [5], zero-valent iron (ZVI) reduction [6], photo [7] or photocatalytic reduction [8], layered double hydroxide reduction [9], advanced reduction processes (ARPs) [10], and so on. Among these technologies, hydrated electron (e_{aq}^-)-based ARPs distinguished themselves in BrO_3^- degradation due to the high rate constants between e_{aq}^- and BrO_3^- ($\sim 10^9 \text{ M}^{-1} \cdot \text{s}^{-1}$) [10,11]; thus, they show potential for their use in household drinking water purifiers, which are characterized by a small hydraulic retention time.

Hydrated electron is one of the most reducing agents (-2.9 V) [12], and it can be generated from the ionizing irradiation of electron beam [13], ultraviolet (UV) activation of sulfite/iodide

(I⁻)/nitriolotriacetic acid [14,15], vacuum-UV irradiation [7], and photoexcitation of organic chromophores [16]. From a practical perspective, the key for—based ARPs is generating e_{aq}⁻ efficiently under ambient conditions. Hydrated electron generation by UV activation of sulfite (UV/sulfite) is promising due to its oxygen self-cleaning property. However, e_{aq}⁻ generation by UV/sulfite was dependent on a high concentration of sulfite and high pH due to the relatively low absorptivity and the protonation of sulfite. Recently, Li et al. [17] proposed a UV/sulfite/I⁻ process to generate e_{aq}⁻, and successfully realized efficient degradation of monochloroacetic acid (12.86 μM·min⁻¹). Enhanced production of e_{aq}⁻ through such a process was based on two facts: (1) both sulfite and I⁻ act as e_{aq}⁻ precursors; (2) sulfite can reduce the e_{aq}⁻ scavenging by reactive iodine species (RIS, e.g., I[•], I₂^{•-}, and I₃⁻). Given the similar rate constant of e_{aq}⁻ toward monochloroacetic acid (1.0 × 10⁹ M⁻¹·s⁻¹ [18]) and BrO₃⁻ (3.4 × 10⁹ M⁻¹·s⁻¹ [10]), it is reasonable to speculate that the UV/sulfite/I⁻ process can also degrade BrO₃⁻ with high efficiency. Yet, to the authors' knowledge, there exist no other reports using this process to degrade BrO₃⁻ under aerobic conditions. Furthermore, the BrO₃⁻ degradation performance using the UV/sulfite/I⁻ process under aerobic conditions, and the possible factors that may affect the degradation efficiency (i.e., pH, anions, and natural organic matter (NOM)) are yet to be investigated.

In this work, we aimed to (1) investigate the reduction efficiency of BrO₃⁻ in prepared water and real water in the UV/sulfite/I⁻ process; (2) explore the mechanism of BrO₃⁻ reduction (role of sulfite/I⁻ and contributors to reduction); (3) identify the transformation product of BrO₃⁻; and (4) evaluate the influence of common water quality parameters (solution temperature, pH, NOM, bicarbonate, and nitrate).

2. Results and Discussion

2.1. Reduction Efficiency of BrO₃⁻ Using UV/Sulfite/I⁻

2.1.1. Degradation Efficiency in Prepared Water

Firstly, a comparison test of UV alone, sulfite/I⁻, UV/I⁻, UV/sulfite, and UV/sulfite/I⁻ processes was conducted to explore the efficiency and advantages of the UV/sulfite/I⁻ process in BrO₃⁻ degradation. To exclude the interference of the water matrix in real water, these comparison experiments were carried out in prepared water (bromate-containing water prepared with deionized water). As shown Figure 1a, under aerobic conditions ([DO]₀ = 7.0 mg·L⁻¹), 10 μM BrO₃⁻ was degraded slowly using the UV/sulfite process or UV/I⁻ process, but completely disappeared within 5 min using the UV/sulfite/I⁻ process at 20 °C. As a comparison, direct UV photolysis and sulfite/I⁻ reduction showed a slow degradation rate, which can be attributed to the weak absorbance at 254 nm for BrO₃⁻ [10] and low reduction potential of sulfite/I⁻ (E(I₂/I⁻) = 0.535 V, and E(S(VI)/S(IV)) = -0.94 V [19]). Figure 1b presents the degradation curves of BrO₃⁻ at different initial concentration ([BrO₃⁻]₀) using the UV/sulfite/I⁻ process. Without exception, BrO₃⁻ concentrations ranging from 0.1–50 μM were completely removed within 10 min. Generally, the BrO₃⁻ degradation rate decreased with increased [BrO₃⁻]₀. Notably, 0.1 μM BrO₃⁻ (World Health Organization (WHO) guideline value) could be degraded thoroughly within 3 min. One can expect a complete removal of BrO₃⁻ in seconds if a UV lamp with higher power (such as 100 W) is used.

Table 1 summarizes the BrO₃⁻ degradation methods previously reported. One can find that the UV/sulfite/I⁻ process is not inferior to any of the previously reported processes. Although the degradation efficiency is dependent on many factors such as reactor geometry and reaction conditions, the crude comparison still indicates the attractive prospect of the UV/sulfite/I⁻ process. Table 2 lists the related reactions in the UV/sulfite/I⁻ system. A preliminary judgment can be made that such a superior degradation efficiency may be attributed to the enhanced formation of e_{aq}⁻/H[•] (No. (1)–(45) in Table 2).

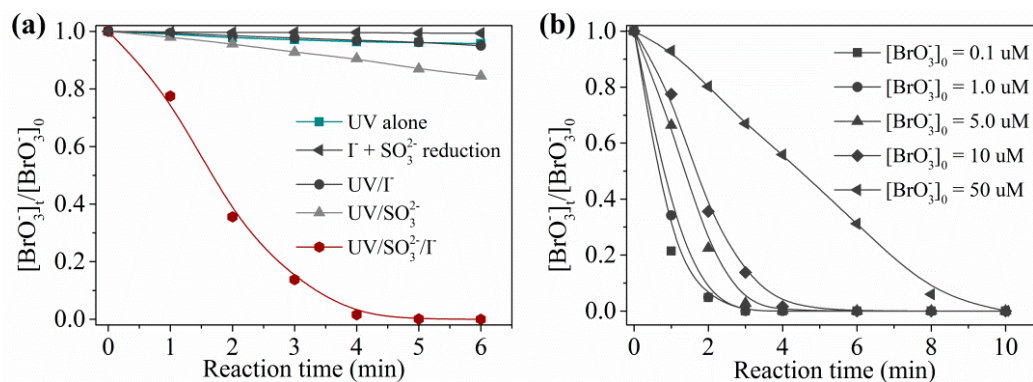


Figure 1. Efficiency of BrO_3^- degradation by ultraviolet (UV)/sulfite/ I^- in prepared water: (a) different processes; (b) different concentrations of BrO_3^- . Conditions: $[\text{I}^-]_0 = 100 \mu\text{M}$, $[\text{sulfite}]_0 = 1.0 \text{ mM}$, $[\text{DO}]_0 = 7.0 \text{ mg}\cdot\text{L}^{-1}$, $\text{pH} = 9.2$, $20 \pm 1 \text{ }^\circ\text{C}$.

Table 1. Comparison of bromate removal efficiency with different processes. UV—ultraviolet; BDD—boron-doped diamond; SCE—saturated calomel electrode; TMP—transmembrane pressure.

Process	Predeoxygenation	$[\text{BrO}_3^-]_0$ ($\text{mg}\cdot\text{L}^{-1}$)	Experimental Conditions	Removal Rate (Time Needed)	Reference
UV ₂₅₄ /sulfite/ I^-	No	0.01	$\text{pH} = 9.2$; $20 \pm 1 \text{ }^\circ\text{C}$; $[\text{I}^-]_0 = 100 \mu\text{M}$, $[\text{sulfite}]_0 = 1.0 \text{ mM}$, $[\text{DO}]_0 = 7.0 \text{ mg}\cdot\text{L}^{-1}$; 10 W	100% (3 min)	This study
UV ₂₅₄ /sulfite	Yes	12.80	$\text{pH} = 7.0$; $23 \text{ }^\circ\text{C}$; $[\text{SO}_3^{2-}]_0 = 1 \text{ mM}$; 10 W	61% (50 min)	[10]
UV-M	Yes	0.60	$\text{pH} = 6.8$; $22\text{--}23 \text{ }^\circ\text{C}$; $2400 \mu\text{W}\cdot\text{cm}^{-2}$	100% (120 min)	[20]
UV-L	Yes	0.50	$\text{pH} = 6.8$; $4900 \mu\text{W}\cdot\text{cm}^{-2}$	100% (250 min)	[21]
UV ₂₅₄ /TiO ₂	No	12.80	$\text{pH} = 1.5\text{--}13.5$; $[\text{TiO}_2] = 0.5 \text{ g}\cdot\text{L}^{-1}$; $1255 \text{ mW}\cdot\text{cm}^{-2}$	100% (90 min)	[22]
UV ₃₆₅ /TiO ₂	No	12.80	$\text{pH} = 1.5\text{--}13.5$; $[\text{TiO}_2] = 0.5 \text{ g}\cdot\text{L}^{-1}$; $1150 \text{ mW}\cdot\text{cm}^{-2}$	78% (180 min)	[22]
Catalyst (4% Pt/SBA-15)	Yes	100.00	$\text{pH} = 6.5$; $25 \text{ }^\circ\text{C}$; catalyst = $30 \text{ mg}\cdot\text{L}^{-1}$	80% (13 min)	[23]
Electrochemical reduction (BDD electrodes)	-	20.00	$\text{pH} = 7.5$; The applied bias potential of -1.0 V (vs. SCE); $[\text{Na}_2\text{SO}_4] = 0.1 \text{ mM}$	90% (2 h)	[24]
Zero-valent iron (ZVI)	Yes	10.00	$\text{pH} = 7$; $20 \text{ }^\circ\text{C}$; $\text{ZVI} = 5 \text{ g}\cdot\text{L}^{-1}$	100% (60 min)	[6]
Acid-washed Zero-valent iron	Yes	10.00	$\text{pH} = 7$; $20 \text{ }^\circ\text{C}$; $\text{ZVI} = 5 \text{ g}\cdot\text{L}^{-1}$, Oxalic acid = $250 \mu\text{M}$	93% (30 min)	[6]
Zn-Fe(II)-Al layered double hydroxides (LDHs)	-	0.10	$\text{pH} = 7$; $22 \text{ }^\circ\text{C}$; Zn-Fe(II)-Al LDHs = $0.50 \text{ g}\cdot\text{L}^{-1}$; mixing rate = 200 rpm	100% (30 min)	[9]
Biological treatment	Yes	5.12	$\text{pH} = 7.1$; $21 \text{ }^\circ\text{C}$; $[\text{SO}_4^{2-}]_0 = 10 \text{ mM}$, with <i>Clostridium</i> and <i>Citrobacter</i> genera bacteria	96% (5 d)	[25]
Hybrid coagulation- nanofiltration	-	2.56	$\text{pH} = 7$; NF-90 membrane (roughness = 388 \AA , zeta potential = -26.5 mV); ionic strength 10 mM as NaCl, TMP 350 kPa	18.9% (9 h)	[26]

Table 2. Summary of related reaction equations during the degradation.

No.	Reactions	Rate Constants ($\text{M}^{-1}\cdot\text{s}^{-1}$)	Reference
1	Sulfite (SO_3^{2-}) + $h\nu \rightarrow \text{SO}_3^{\bullet-} + e_{\text{aq}}^-$	-	[27,28]
2	$\text{HSO}_3^- + h\nu \rightarrow \text{SO}_3^{\bullet-} + \text{H}^\bullet$	-	[27,28]
3	$\text{SO}_3^{\bullet-} + \text{SO}_3^{\bullet-} \rightarrow \text{S}_2\text{O}_6^{2-}$	1.8×10^8	[27,29]
4	$\text{SO}_3^{\bullet-} + \text{SO}_3^{\bullet-} + \text{H}_2\text{O} \rightarrow \text{SO}_4^{2-} + \text{SO}_3^{2-} + 2\text{H}^+$	3.2×10^8	[27,29]

Table 2. Cont.

No.	Reactions	Rate Constants (M ⁻¹ ·s ⁻¹)	Reference
5	SO ₃ ²⁻ + HO• → SO ₃ ^{•-} + OH ⁻	5.5 × 10 ⁹	[12]
6	I ⁻ + hν → I• + e _{aq} ⁻	-	[30]
7	I ⁻ + I• ↔ I ₂ ^{•-}	> 1.2 × 10 ⁴	[31]
8	I• + I• ↔ I ₂	1.0 × 10 ¹⁰	[31]
9	I• + I ₂ ⁻ → I ₃ ⁻	≥ 6.4 × 10 ⁹	[32]
10	I ₂ ^{•-} + I ₂ ⁻ → I ₃ ⁻ + I ⁻	3.2 × 10 ⁹	[32]
11	I ₂ + I ⁻ ↔ I ₃ ⁻	7.2 × 10 ²	[32]
12	e _{aq} ⁻ + I ₂ → I ₂ ^{•-}	5.3 × 10 ¹⁰	[33]
13	I• + SO ₃ ²⁻ → I ⁻ + SO ₃ ^{•-}	1.4 × 10 ⁹	[31]
14	I• + HSO ₃ ⁻ → I ⁻ + H ⁺ + SO ₃ ^{•-}	6.3 × 10 ⁸	[31]
15	I ₂ ^{•-} + HSO ₃ ⁻ → 2I ⁻ + H ⁺ + SO ₃ ^{•-}	1.1 × 10 ⁸	[34]
16	I ₂ ^{•-} + SO ₃ ²⁻ → 2I ⁻ + SO ₃ ^{•-}	1.9 × 10 ⁸	[34]
17	I ₃ ⁻ + SO ₃ ²⁻ → 2I ⁻ + ISO ₃ ^{•-}	2.9 × 10 ⁸	[35]
18	I ₃ ⁻ + HSO ₃ ⁻ → 2I ⁻ + H ⁺ + ISO ₃ ^{•-}	1.5 × 10 ⁷	[35]
19	I ₂ + HSO ₃ ⁻ → I ⁻ + ISO ₃ ^{•-} + H ⁺	1.7 × 10 ⁹	[35]
20	I ₂ + SO ₃ ²⁻ → I ⁻ + ISO ₃ ^{•-}	3.1 × 10 ⁹	[35]
21	ISO ₃ ⁻ + H ₂ O → I ⁻ + SO ₄ ²⁻ + 2H ⁺	-	[35]
22	I ⁻ + H ₂ O + hν → I ⁻ H ₂ O*	-	[30]
23	I ⁻ H ₂ O* → (I•, e ⁻) + H ₂ O	-	[30]
24	(I•, e ⁻) → I• + e _{aq} ⁻	-	[30]
25	e _{aq} ⁻ + I ₂ → 2I ⁻	9.0 × 10 ¹⁰	[12]
26	e _{aq} ⁻ + I ₃ ⁻ → I ⁻ + I ₂ ⁻	3.5 × 10 ¹⁰	[32]
27	e _{aq} ⁻ + I ₂ → I ₂ ^{•-}	5.3 × 10 ¹⁰	[32]
28	H• + I ₂ ↔ H ⁺ + I ₂ ^{•-}	3.5 × 10 ¹⁰	[32]
29	H• + I ₂ ⁻ ↔ H ⁺ + 2I ⁻	1.8 × 10 ⁷	[12]
30	H• + I ₃ ⁻ ↔ H ⁺ + I• + 2I ⁻	2.0 × 10 ¹⁰	[32]
31	e _{aq} ⁻ + e _{aq} ⁻ → H ₂ O + 2OH ⁻	5.5 × 10 ⁹	[12]
32	e _{aq} ⁻ + H• → H ₂ + OH ⁻	2.5 × 10 ¹⁰	[12]
33	e _{aq} ⁻ + H ⁺ → H•	2.3 × 10 ¹⁰	[12]
34	e _{aq} ⁻ + H ₂ O → H• + OH ⁻	19	[12]
35	H• + OH ⁻ → e _{aq} ⁻ + H ₂ O	2.2 × 10 ⁷	[12]
36	e _{aq} ⁻ + HSO ₃ ⁻ → H• + SO ₃ ^{•-}	2.0 × 10 ⁷	[36]
37	H• + H ₂ O → H ₂ + HO•	10	[12]
38	H• + H• → H ₂	7.8 × 10 ⁹	[12]
39	e _{aq} ⁻ + SO ₃ ^{•-} → SO ₃ ²⁻	5.8 × 10 ⁹	[29]
40	H• + SO ₃ ^{•-} → HSO ₃ ⁻	slow	[27]
41	e _{aq} ⁻ + SO ₃ ²⁻ → OH ⁻ + HSO ₃ ²⁻	< 1.5 × 10 ⁶	[12]
42	H• + HSO ₃ ⁻ → H ₂ + SO ₃ ^{•-}	2 × 10 ⁴	[27]
43	S ₂ O ₆ ²⁻ + e _{aq} ⁻ → SO ₃ ²⁻ + SO ₃ ^{•-}	2 × 10 ⁵	[27]
44	S ₂ O ₆ ²⁻ + H• → HSO ₃ ⁻ + SO ₃ ^{•-}	2 × 10 ⁵	[27]
45	HSO ₃ ⁻ + SO ₃ ^{•-} → S ₂ O ₆ ²⁻ + H•	slow	[27]
46	O ₂ + e _{aq} ⁻ → O ₂ ^{•-}	1.9 × 10 ¹⁰	[12]
47	O ₂ + H• → HO ₂ [•] ↔ H ⁺ + O ₂ ^{•-}	1.2 × 10 ¹⁰	[12]
48	HCO ₃ ⁻ + e _{aq} ⁻ → CO ₃ ^{•-} + OH ⁻	< 1.0 × 10 ⁶	[12]
49	HCO ₃ ⁻ + I• → CO ₃ ^{•-} + I ⁻ + H ⁺	-	[37]
50	NO ₂ ⁻ + e _{aq} ⁻ → (NO ₂ ^{•-}) ²⁻	4.1 × 10 ⁹	[12]
51	NO ₂ ⁻ + H• → NO• + OH ⁻	7.1 × 10 ⁸	[12]
52	CH ₂ ClCOO ⁻ + e _{aq} ⁻ → •CH ₂ COO ⁻ + Cl ⁻	1.0 × 10 ⁹	[17]
53	CH ₂ ClCOO ⁻ + H• → •CHClCOO + H ₂	3.6 × 10 ⁶	[17]
54	N ₂ O + e _{aq} ⁻ → N ₂ + HO• + OH ⁻	9.1 × 10 ⁹	[12]
55	N ₂ O + H• → N ₂ + HO•	2.1 × 10 ⁶	[12]
56	CO ₃ ^{•-} + I ⁻ → CO ₃ ²⁻ + I•	1.3 × 10 ⁸	[38]
57	CO ₃ ^{•-} + SO ₃ ²⁻ → CO ₃ ²⁻ + SO ₃ ^{•-}	1.0 × 10 ⁷	[39]

2.1.2. Validation of UV/Sulfite/I⁻ Process with Real Water

To evaluate the potential for practical water treatment, we also investigated the degradation efficiency of BrO₃⁻ with four different tap waters (TP1, TP2, TP3, and TP4) using UV/sulfite/I⁻ process (Figure 2). The water quality parameters of four real waters are listed in Table S1 (Supplementary Materials). These four tap waters were collected from four different cities of Eastern China. Their pH values were nearly the same, but the other parameters (dissolved organic carbon (DOC), HCO₃⁻, Cl⁻, NO₃⁻, and SO₄²⁻) were quite different. The degradation efficiency of BrO₃⁻ with the four authentic waters suffered some degree of decrease compared to that in pure water. For a UV dosage of 231.38 mJ·cm⁻² (typical UV dosage for virus inactivation is

40–100 $\text{mJ}\cdot\text{cm}^{-2}$ [40]), the degradation rates of BrO_3^- for the four tap waters were 91%, 88%, 85%, and 67%. Such results indicated that the degradation efficiency varied with changes in the water matrix. Over all, the degradation process of BrO_3^- in real water using UV/sulfite/ I^- was also satisfactory. These results powerfully confirm that BrO_3^- reduction with the UV/sulfite/ I^- process in real water is still efficient.

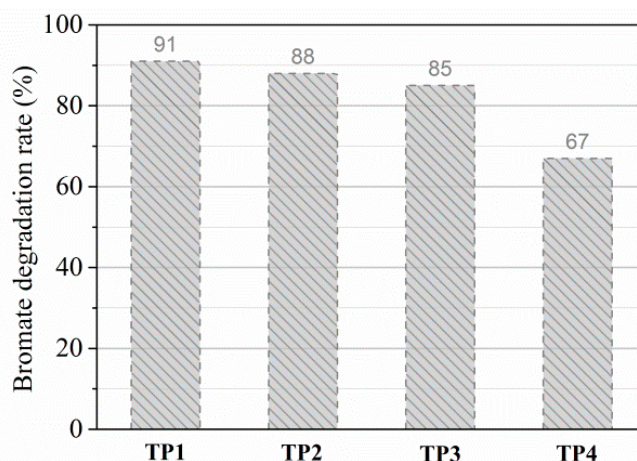


Figure 2. Efficiencies of BrO_3^- degradation using UV/sulfite/ I^- in real water. Conditions: $[\text{BrO}_3^-]_0 = 10 \mu\text{M}$, $[\text{I}^-]_0 = 100 \mu\text{M}$, $[\text{sulfite}]_0 = 1.0 \text{ mM}$, UV dosage = $231.38 \text{ mJ}\cdot\text{cm}^{-2}$.

2.2. Mechanism of BrO_3^- Reduction

2.2.1. Main Contributor to BrO_3^- Reduction

Hydrated electrons and H^\bullet were certified as the main reductive reactive species in the UV/sulfite/ I^- process [17]. As e_{aq}^- and H^\bullet are a conjugated acid–base pairs and both of them showed high reactivity toward BrO_3^- ($k(\text{e}_{\text{aq}}^- + \text{BrO}_3^-) = 3.4 \times 10^9 \text{ M}^{-1}\cdot\text{s}^{-1}$ [10]; $k(\text{H}^\bullet + \text{BrO}_3^-) = 2.0 \times 10^7 \text{ M}^{-1}\cdot\text{s}^{-1}$ [41]), which of the two dominated BrO_3^- reduction needed clarification. Monochloroacetic acid (MCAA) and nitrite (NO_2^-) were used as radical scavengers to explore the contributions of e_{aq}^- and H^\bullet (No. (50)–(53) in Table 2). As shown in Figure 3, the presence of (scavenger for e_{aq}^- and H^\bullet) yielded a degradation rate of $0.31 \mu\text{M}\cdot\text{min}^{-1}$, while presence of MCAA (scavenger for e_{aq}^-) generated a degradation rate of $0.59 \mu\text{M}\cdot\text{min}^{-1}$. Based on the rate constant for the case without scavenger addition ($2.61 \mu\text{M}\cdot\text{min}^{-1}$), contributions for e_{aq}^- and H^\bullet were calculated to be 77.4% and 10.7%, respectively, under current conditions.

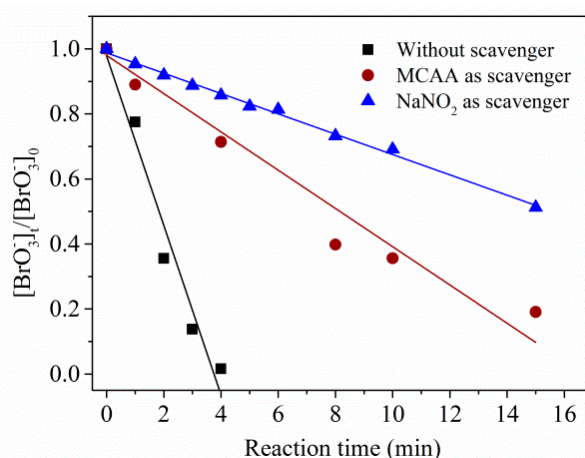


Figure 3. Degradation of BrO_3^- using UV/sulfite/ I^- process in the presence of monochloroacetic acid (MCAA) and NO_2^- . Conditions: $[\text{BrO}_3^-]_0 = 10 \mu\text{M}$, $[\text{I}^-]_0 = 100 \mu\text{M}$, $[\text{sulfite}]_0 = 1.0 \text{ mM}$, $[\text{MCAA}]_0 = 1.0 \text{ mM}$, $[\text{NO}_2^-]_0 = 4.0 \text{ mM}$, $[\text{DO}]_0 = 7.0 \text{ mg}\cdot\text{L}^{-1}$, $\text{pH} = 9.2$, $20 \pm 1 \text{ }^\circ\text{C}$.

2.2.2. The Role of I^- and Sulfite

By fitting the degradation curves of BrO_3^- using the UV/sulfite/ I^- process, pseudo zero-order kinetics was found to be followed. Figure 4a shows that BrO_3^- degradation improved with increased $[sulfite]_0$. Figure 4b reveals three distinct phases for the influence of sulfite dosage. The degradation rate of BrO_3^- (r) accelerated slightly from $\sim 0.10 \mu M \cdot min^{-1}$ to $0.12 \mu M \cdot min^{-1}$ (phase I) by 0.5 mM sulfite, and a further increase of sulfite concentration caused a remarkable linear enhancement (phase II). However, much higher sulfite dosage (1.5–2.0 mM) only brought subtle increases of rate constants (phase III), which may be explained by the fact that incident photons were in short supply and obvious self-quenching of radicals occurred.

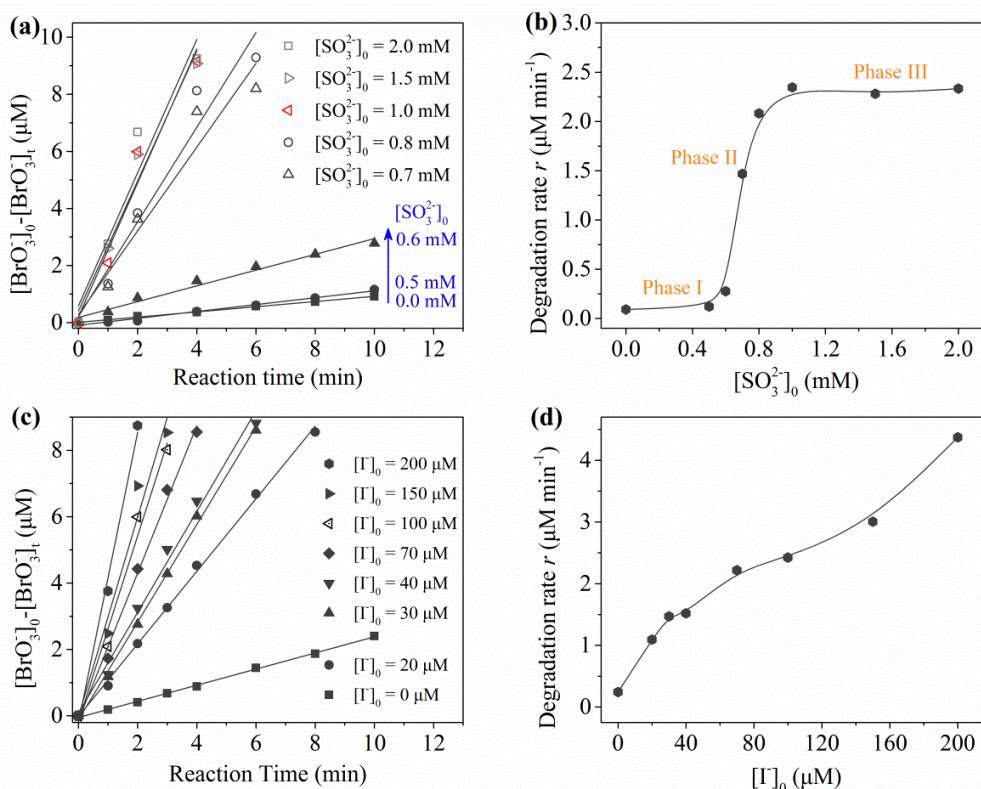


Figure 4. Degradation of BrO_3^- using UV/sulfite/ I^- process: (a) effects of sulfite dosage ($[I^-]_0 = 100 \mu M$); (b) degradation rate constant (r) vs. $[sulfite]_0$; (c) effects of I^- dosage; (d) degradation rate constant (r) vs. $[I^-]_0$. Conditions: $[BrO_3^-]_0 = 10 \mu M$, pH = 9.2, $[DO]_0 = 7.0 \text{ mg} \cdot \text{L}^{-1}$, $20 \pm 1 \text{ }^\circ\text{C}$.

Regarding the role of I^- , one can find that a concentration change at the 10 μM level would result in a significant variation in degradation efficiency of BrO_3^- (Figure 4c). Comparing the two linear relationships in Figure 4b,d, the degradation efficiency was about 5.6 times (normalized to molar concentration) more dependent on than on sulfite. Thus, I^- may play an important role in the process. Figure 5 presents the simultaneous evolution of sulfite and I^- during the degradation of BrO_3^- . Sulfite decreased rapidly within the first 2 min and then slowly depleted, while I^- almost stayed constant as long as sulfite was available. The UV photolysis mechanism of I^- is shown in No. (6)–(12) in Table 2. Iodide was a stronger UV-absorber at 254 nm compared to sulfite and had a higher quantum yield than sulfite [17]. However, the UV/ I^- process failed to show superior reduction efficiency compared to the UV/sulfite process due to the scavenging effect of e_{aq}^- by the photogenerated RISs and self-consumption of I^- (No. (5)–(14) in Table 2). The nearly constant concentration of I^- indicated that the presence of sulfite may inhibit negative effects of RISs and promote the regeneration of I^- . Based on the above discussion, one can conclude that I^- mainly served as an e_{aq}^- precursor, while sulfite not only

played a role as an e_{aq}^- precursor, but also as an RIS shielding agent and a regenerant of I^- . Considering the negligible chemical change of I^- during the whole reaction, I^- acted similarly to a catalyst.

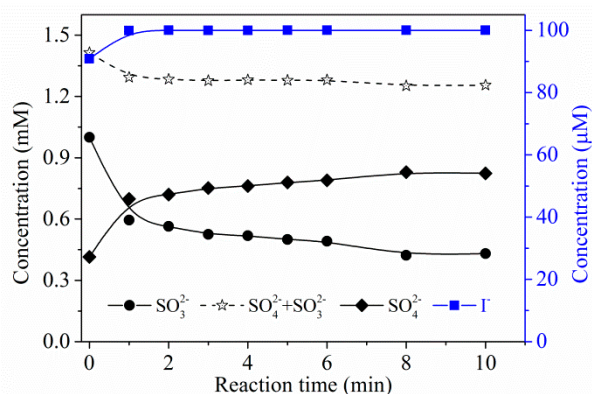


Figure 5. Mass balance of sulfur and iodine during degradation of BrO_3^- using UV/sulfite/ I^- process. Conditions: $[BrO_3^-]_0 = 10 \mu M$, $[I^-]_0 = 100 \mu M$, $[sulfite]_0 = 1.0 \text{ mM}$, $[DO]_0 = 7.0 \text{ mg}\cdot\text{L}^{-1}$, $\text{pH} = 9.2$, $20 \pm 1 \text{ }^\circ\text{C}$.

2.2.3. Transformation Products of BrO_3^-

Transformation products of BrO_3^- ($10 \mu M$) treated by combining 1 mM sulfite and $100 \mu M$ I^- at $\text{pH} 9.2$ under 254-nm UV irradiation were monitored, and the results are shown in Figure 6. For the prepared water, all BrO_3^- converted to Br^- during degradation without other bromine-containing substances. No other inorganic bromine-containing substances, such as BrO^- / $HBrO$, were detected. This could be proven by the Br^- yield per μM BrO_3^- degradation ($k_0 = 1.0$). We also tested the BrO_3^- degradation products in four tap waters (Figure 6), and a similar phenomenon was observed. These results declared that e_{aq}^- -based reduction initiated with the UV/sulfite/ I^- process was an efficient method of removing BrO_3^- .

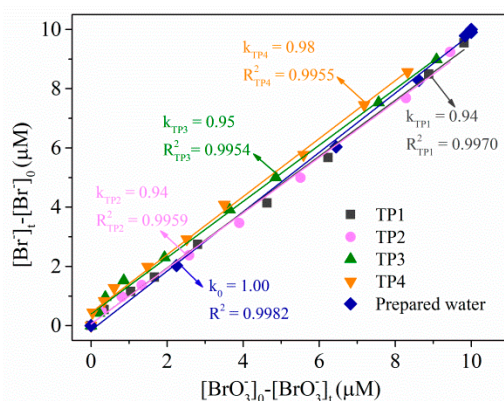


Figure 6. Transformation products analysis of BrO_3^- in prepared water and four tap waters using the UV/sulfite/ I^- process. Conditions: $[BrO_3^-]_0 = 10 \mu M$, $[I^-]_0 = 100 \mu M$, $[sulfite]_0 = 1.0 \text{ mM}$, $[DO]_0 = 7.0 \text{ mg}\cdot\text{L}^{-1}$, $\text{pH} = 9.2$, $20 \pm 1 \text{ }^\circ\text{C}$.

2.3. Influence of Water Quality Parameters

As stated above, the water matrix presented non-negligible effects on BrO_3^- degradation using the UV/sulfite/ I^- process. How the water matrix influences the degradation process is of great concern. Thus, the effects on individual common water quality parameters were investigated one by one.

Taking into consideration the temperature fluctuation of drinking water, the degradation efficiency under different temperatures ranging from $9\text{--}38 \text{ }^\circ\text{C}$ was investigated (Figure 7a). When the solution temperature changed from 8.9 to $38 \text{ }^\circ\text{C}$, the degradation rate increased about fivefold. It should be noted that, even at a relatively low temperature ($8.9 \text{ }^\circ\text{C}$), BrO_3^- could still be degraded thoroughly

within 10 min. According to van 't Hoff's law, a temperature increase of 30 °C will lead to an 8–64-fold increase in reaction rate. Thus, the degradation process was not entirely thermodynamically controlled. In addition, based on the degradation data under different temperatures, the apparent activation energy of BrO_3^- in the UV/sulfite/ I^- process was calculated ($E_a = 34.55 \text{ kJ}\cdot\text{mol}^{-1}$; Figure S1, Supplementary Materials). This low apparent activation energy reasonably explained the efficient degradation of BrO_3^- .

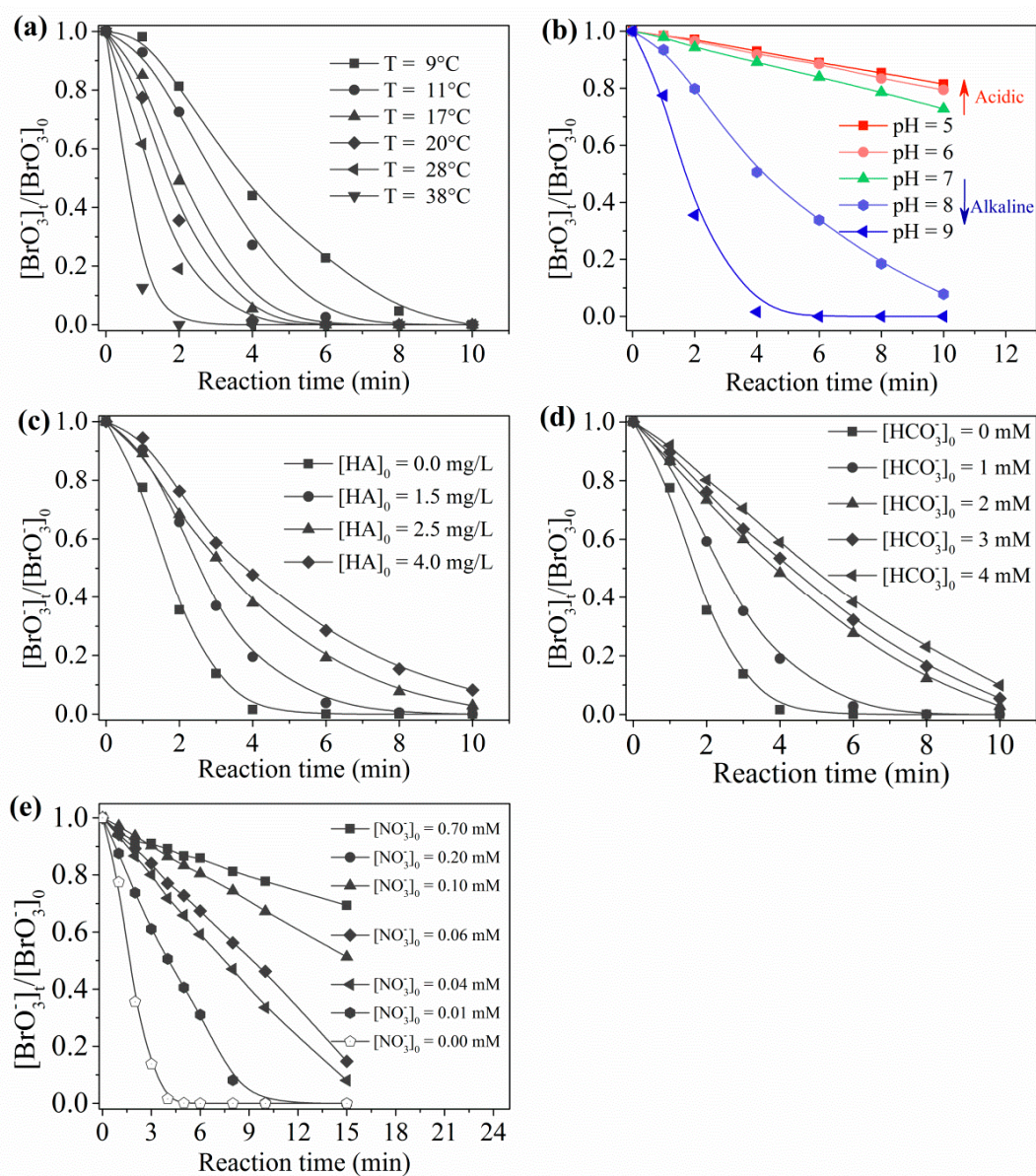


Figure 7. Influence on water quality parameters with regards to the degradation of BrO_3^- using the UV/sulfite/ I^- process: (a) temperature; (b) pH; (c) humic acid (HA); (d) HCO_3^- ; (e) NO_3^- . Conditions: $[\text{BrO}_3^-]_0 = 10 \mu\text{M}$, $[\text{I}^-]_0 = 100 \mu\text{M}$, $[\text{sulfite}]_0 = 1.0 \text{ mM}$, $[\text{DO}]_0 = 7.0 \text{ mg}\cdot\text{L}^{-1}$, $\text{pH} = 9.2$, $20 \pm 1 \text{ }^\circ\text{C}$.

Figure 7b shows the effect of pH on BrO_3^- reduction. Increased pH improved the degradation of BrO_3^- and the improvement became especially remarkable when the pH was raised above 7. Photolysis of I^- was almost not influenced by pH change [30]. Solution pH plays a significant role in the distribution ratio of $\text{SO}_3^{2-}/\text{S(IV)}$ and the interconversion between H^\bullet and e_{aq}^- [14,18]. As regards S(IV) species, HSO_3^- is dominant at pH 3–7, while SO_3^{2-} becomes dominant at $\text{pH} > 7$ [42,43]. Given that e_{aq}^- was mainly produced due to the UV activation of SO_3^{2-} rather than HSO_3^- (No. (1) and (2)) and that e_{aq}^- was the main contributor to BrO_3^- , one can easily understand why the alkaline environment

benefited the degradation process. In addition, high pH promoted the conversion of H^\bullet to e_{aq}^- (No. (33) and (34)). Thus, pH exerted its influence through changing the SO_3^{2-} fraction and the interconversion of H^\bullet and e_{aq}^- .

Humic acid (HA) was used as a representative of NOM herein. A concentration range of 1.5–4.0 $mg \cdot L^{-1}$ HA was dosed in the reaction process to assess its influence (Figure 7c). It is well known that excitation of HA by UV can produce reactive species such as excited triplet states of HA and hydroxyl radicals [44]. These oxidative reactive species can compete with BrO_3^- for e_{aq}^- , which slowed BrO_3^- degradation. HA also competed for incident photons (inner filter effect) with sulfite/ I^- , which may have affected the generation of e_{aq}^- . The results in Figure 7c confirmed these speculations. Overall, the removal rate of BrO_3^- decreased with an increase in HA concentration; 4.0 $mg \cdot L^{-1}$ HA resulted in a removal rate decrease from 98.5% to 41% (4 min reaction time). Thus, HA was confirmed as a strong inhibitor for the degradation of BrO_3^- using UV/sulfite/ I^- .

Figure 7d displays the influence of bicarbonate (HCO_3^-) on the degradation process. Bicarbonate at an environmentally relevant concentration level (1–4 mM) caused obvious inhibition effects. Specifically, 1 mM and 2 mM HCO_3^- resulted in a degradation rate decrease by about 20% and 50%, respectively. Nevertheless, a further increase in HCO_3^- concentration (3–4 mM) only brought about an extra 3–5% inhibition. The rate constant of HCO_3^- with e_{aq}^- ($<1.0 \times 10^6 M^{-1} \cdot s^{-1}$ [45]) is much lower than that of BrO_3^- with e_{aq}^- ($3.0 \times 10^9 M^{-1} \cdot s^{-1}$ [10]). Thus, 1.0–4.0 mM HCO_3^- produced an e_{aq}^- scavenging rate of $<(1.0\text{--}4.0) \times 10^3 s^{-1}$, while 10 μM BrO_3^- produced an e_{aq}^- scavenging rate of $3.0 \times 10^4 s^{-1}$. From the point of view of competitive kinetics, 1.0–4.0 mM HCO_3^- would confer a subtle influence on BrO_3^- degradation. On the other hand, e_{aq}^- can react with HCO_3^- to generate oxidative $CO_3^{\bullet-}$ (No. (48)), and the formed $CO_3^{\bullet-}$ will compete for sulfite with RIS (No. (48)). Such a competitive effect undoubtedly interfered with the cycle of I^- . Given the important role of I^- , a deteriorating degradation performance was expected. Hence, unlike the case using the UV/sulfite system, the effect of HCO_3^- could not be ignored in the UV/sulfite/ I^- process.

Nitrate (NO_3^-), a common water matrix component, is a strong electron scavenger (No. (52)) and, thus, its influence was explored (Figure 7e). Due to fast reaction kinetics, the degradation of BrO_3^- was greatly inhibited by the presence of just 0.01 mM NO_3^- (0.14 mg/L as N). Existence of 0.7 mM NO_3^- (United States Environmental Protection Agency (USEPA) guideline value) produced 90% inhibition, suggesting that NO_3^- elimination to an acceptable level was necessary for BrO_3^- control using the UV/sulfite/ I^- process.

3. Materials and Methods

3.1. Materials

Sodium sulfite, KI, HA, $NaNO_3$, $NaNO_2$, MCAA, atrazine (ATZ), and $NaBrO_3$ were American Chemical Society (ACS) reagent grade and were purchased from Sigma-Aldrich (San Francisco, CA, USA). Sodium bicarbonate, H_2O_2 , and H_2SO_4 were analytic reagent (AR) grade and were obtained from Sinopharm Chemical Reagents (Shanghai, China). Boracic acid (ACS reagent, 99.5%) and $Na_2B_4O_7 \cdot H_2O$ (ACS reagent, 99.5%) were purchased from J&K Scientific Ltd, while D-mannitol (AR reagent, 98.0%) was purchased from Macklin (Shanghai, China). Glass-fiber filters (0.45 μm) were ordered from Millipore (London, UK). HA stock solution was prepared in a procedure similar to that described in our previous work [10]. The concentration of the HA stock solution was calibrated using a total organic carbon (TOC)-VCPH analyzer (Shimadzu, Japan). Unless otherwise specified, all fresh stock solutions were prepared with 18.2 $M\Omega \cdot cm$ ultrapure water. Four different tap waters were collected from four different cities located in east China and were dechlorinated before use.

3.2. Experimental Procedure

An 800-mL cylindrical glass photoreactor was used to conduct the experiments, and the reaction volume was 500 mL. A Heraeus low-pressure UV lamp (10W, ozone-free, light centered at 254 nm, Hanau, Germany)

was used, and D-mannitol (3%) was used to fix sulfite ions before detecting. The pH of the reaction solution was adjusted with 0.2 M borate buffer and/or 0.1 M·H₂SO₄. Other than the experiments to evaluate the impact of pH, the solution pH was set at 9.2 to guarantee the valid concentration of sulfite. The constant temperature (10–40 °C) of reaction solution was controlled using a thermostat bath. The UV lamp was preheated for 10 min to ensure achieving a stable output prior to experiment start. Samples were drawn at predetermined time intervals and quenched with H₂O₂ before analysis. In addition, all experiments were carried out under aerobic conditions without deoxygenation.

3.3. Analytical Methods

Solution pH was measured using a portable pH meter (Orion 3-Star, Thermo Scientific, MA, USA). Bromate, SO₃²⁻, SO₄²⁻, I⁻, Br⁻, NO₃⁻, NO₂⁻, and Cl⁻ were analyzed using ion chromatography (Dionex ICS-2000, Chameleon 6.8, Sunnyvale, CA, USA) in isocratic elution mode (20 mM and 50 mA suppressor current). The BrO⁻/HBrO was analyzed using the diethyl-*p*-phenylenediamine colorimetric method [46]. Atrazine was detected with a high-performance liquid chromatograph equipped with a XDB-C18 column (5 μm × 4.6 mm × 150 mm). The eluent was 40% water and 60% methanol and run at 1 mL·min⁻¹. Bicarbonate was detected using chemical titration with a standard HCl solution, and cesium chloride was first added to deposit SO₄²⁻ and SO₃²⁻ before titration [47].

3.4. UV Intensity and UV Fluence Calculation

Considering the actual output loss of the lamp, the effective ultraviolet dosage was calibrated with atrazine as an exposure agent [48]. The photon fluence was determined to be 4.5×10^{-7} Einstein·s⁻¹. The effective optical path length (14.77 cm) was determined using H₂O₂ as an exposure agent. The UV dosage was calculated to be 0.0964 mW·cm⁻².

4. Conclusions

This study examined the potential of an iodide-assisted UV/sulfite process (UV/Sulfite/I⁻) for the degradation of BrO₃⁻ in drinking water. The results indicated that UV/Sulfite/I⁻ showed much faster reaction kinetics in an aerobic environment than other methods reported. Competitive kinetic experiments demonstrated that BrO₃⁻ degradation was mainly achieved due to e_{aq}⁻ reduction (77.4% contribution). With respect to the roles of sulfite and I⁻, both acted as e_{aq}⁻ precursors, and sulfite was involved in the regeneration of I⁻. Given the unvaried concentration of I⁻, I⁻ was considered to play a catalyst-like role. Bromide was the only transformation product of BrO₃⁻ even in the presence of background in tap water. The investigation on the influence of common water quality parameters revealed that UV/Sulfite/I⁻ was especially sensitive to nitrate, 0.04 mM of which resulted in ~50% inhibition of BrO₃⁻ reduction. The solution pH exerted its influence through adjusting the valid concentration of sulfite. Bicarbonate and HA at an environment relevant level caused moderate inhibition. Overall, UV/Sulfite/I⁻ is promising for practical treatment of BrO₃⁻-polluted drinking water, and pretreatment to reduce nitrate is suggested prior to application.

Supplementary Materials: The following are available online at <http://www.mdpi.com/2073-4344/8/12/652/s1>: Figure S1: Determination of activation energy of BrO₃⁻ degradation in the UV/sulfite/I⁻ process; Table S1: Water quality parameters of four tap waters.

Author Contributions: Conceptualization, X.L.; data curation, J.W. and X.L.; formal analysis, T.Z., J.W., D.Y., and L.W.; project administration, T.Z.; writing—original draft, J.W.; writing—review and editing, X.L.; Y.S. contributed reagents/materials/analysis tools.

Acknowledgments: This research was funded by the special S&T project on the treatment and control of water pollution (Grant No. 2017ZX07201-003), the Natural Science Foundation of Zhejiang Province (Grant No. LQ19E080023), the Major International (Regional) Joint Research Program of China (Grant No. 51761145022), and the National Key Research and Development Program of China (No. 2016YFC0400601, 2016YFC0400606). The authors greatly thank Luo, F. for his discussion and suggestion.

Conflicts of Interest: The authors declare no conflicts of interest.

References

1. Krasner, S.W.; Glaze, W.H.; Weinberg, H.S.; Daniel, P.A.; Najm, I.N. Formation and control of bromate during ozonation of waters containing bromide. *Water Res.* **1993**, *85*, 73–81. [[CrossRef](#)]
2. Huang, X.; Gao, N.; Lu, P. Bromate reduction by granular activated carbon. *Environ. Sci.* **2007**, *28*, 2264–2269. [[CrossRef](#)]
3. Wang, L.; Batchelor, B.; Pillai, S.D.; Botlaguduru, V.S.V. Electron beam treatment for potable water reuse: Removal of bromate and perfluorooctanoic acid. *Chem. Eng. J.* **2016**, *302*, 58–68. [[CrossRef](#)]
4. Merle, T.; Pronk, W.; Gunten, U.V. MEMBRO₃X, a novel combination of a membrane contactor with advanced oxidation (O₃/H₂O₂) for simultaneous micropollutant abatement and bromate minimization. *Environ. Sci. Technol. Lett.* **2017**, *4*, 180–185. [[CrossRef](#)]
5. Kirisits, M.J.; Snoeyink, V.L.; Inan, H.; Chee-sanford, J.C.; Raskin, L.; Brown, J.C. Water quality factors affecting bromate reduction in biologically active carbon filters. *Water Res.* **2001**, *35*, 891–900. [[CrossRef](#)]
6. Lin, K.A.; Lin, C.H. Enhanced reductive removal of bromate using acid-washed zero-valent iron in the presence of oxalic acid. *Chem. Eng. J.* **2017**, *325*, 144–150. [[CrossRef](#)]
7. Gonzalez, M.G.; Oliveros, E.; Wörner, M.; Braun, A.M. Vacuum-ultraviolet photolysis of aqueous reaction systems. *J. Photoch. Photobiol. C* **2004**, *5*, 225–246. [[CrossRef](#)]
8. Noguchi, H.; Nakajima, A.; Watanabe, T.; Hashimoto, K. Removal of bromate ion from water using TiO₂ and alumina-loaded TiO₂ photocatalysts. *Water Sci. Technol.* **2002**, *46*, 27–31. [[CrossRef](#)]
9. Zhang, Y.; Jing, S.; Liu, H. Reactivity and mechanism of bromate reduction from aqueous solution using Zn–Fe(II)–Al layered double hydroxides. *Chem. Eng. J.* **2015**, *266*, 21–27. [[CrossRef](#)]
10. Liu, X.; Zhang, T.; Shao, Y. Aqueous bromate reduction by UV activation of sulfite. *Clean-Soil Air Water* **2015**, *42*, 1370–1375. [[CrossRef](#)]
11. Xiao, Q.; Yu, S.; Li, L.; Wang, T.; Liao, X.; Ye, Y. An overview of advanced reduction processes for bromate removal from drinking water: Reducing agents, activation methods, applications and mechanisms. *J. Hazard. Mater.* **2017**, *324*, 230–240. [[CrossRef](#)]
12. Buxton, G.V.; Greenstock, C.L.; Helman, W.P.; Ross, A.B. Critical review of rate constants for reactions of hydrated electrons, hydrogen atoms and hydroxyl radicals ($\cdot\text{OH}/\cdot\text{O}^-$) in aqueous solution. *J. Phys. Chem. Ref. Data* **1988**, *17*, 513–886. [[CrossRef](#)]
13. Jones, C.G.; Silverman, J.; Al-Sheikhly, M.; Neta, P.; Poster, D.L. Dechlorination of polychlorinated biphenyls in industrial transformer oil by radiolytic and photolytic methods. *Environ. Sci. Technol.* **2003**, *37*, 5773–5777. [[CrossRef](#)] [[PubMed](#)]
14. Liu, X.; Zhang, T.; Wang, L.; Shao, Y.; Fang, L. Hydrated electron-based degradation of atenolol in aqueous solution. *Chem. Eng. J.* **2015**, *260*, 740–748. [[CrossRef](#)]
15. Sun, Z.; Zhang, C.; Xing, L.; Zhou, Q.; Dong, W.; Hoffmann, M.R. UV/nitritotriacetic acid process as a novel strategy for efficient photoreductive degradation of perfluorooctanesulfonate. *Environ. Sci. Technol.* **2018**, *52*, 2953–2962. [[CrossRef](#)] [[PubMed](#)]
16. Gu, J.; Ma, J.; Jiang, J.; Yang, L.; Yang, J.; Zhang, J.; Chi, H.; Song, Y.; Sun, S.; Tian, W.Q. Hydrated electron (e_{aq}^-) generation from phenol/UV: Efficiency, influencing factors, and mechanism. *Appl. Catal. B. Environ.* **2017**, *200*, 585–593. [[CrossRef](#)]
17. Yu, K.; Li, X.; Chen, L.; Fang, J.; Chen, H.; Li, Q.; Chi, N.; Ma, J. Mechanism and efficiency of contaminant reduction by hydrated electron in the sulfite/iodide/UV process. *Water Res.* **2017**, *129*, 357–364. [[CrossRef](#)] [[PubMed](#)]
18. Li, X.; Ma, J.; Liu, G.; Fang, J.; Yue, S.; Guan, Y.; Chen, L.; Liu, X. Efficient reductive dechlorination of monochloroacetic acid by sulfite/UV process. *Environ. Sci. Technol.* **2012**, *46*, 7342–7349. [[CrossRef](#)] [[PubMed](#)]
19. Bard, E.B.; Parsons, R.; Jordan, J. *Standard Potentials in Aqueous Solution*; Routledge: New York, NY, USA, 1985.
20. Bensalah, N.; Liu, X.; Abdelwahab, A. Bromate reduction by ultraviolet light irradiation using medium pressure lamp. *Int. J. Environ. Stud.* **2013**, *70*, 566–582. [[CrossRef](#)]
21. Jung, B.; Nicola, R.; Batchelor, B.; Abdel-Wahab, A. Effect of low- and medium-pressure Hg UV irradiation on bromate removal in advanced reduction process. *Chemosphere* **2014**, *117*, 663–672. [[CrossRef](#)]
22. Zhang, X.; Zhang, T.; Ng, J.; Pan, J.; Sun, D. Transformation of bromine species in TiO₂ photocatalytic system. *Environ. Sci. Technol.* **2010**, *44*, 439–444. [[CrossRef](#)] [[PubMed](#)]

23. Zhang, Z.; Luo, Y.; Guo, Y.; Shi, W.; Wang, W.; Zhang, B.; Zhang, R.; Bao, X.; Wu, S.; Cui, F. Pd and Pt nanoparticles supported on the mesoporous silica molecular sieve SBA-15 with enhanced activity and stability in catalytic bromate reduction. *Chem. Eng. J.* **2018**, *344*, 114–123. [[CrossRef](#)]
24. Zhao, X.; Liu, H.; Li, A.; Shen, Y.; Qu, J. Bromate removal by electrochemical reduction at boron-doped diamond electrode. *Electrochim. Acta* **2012**, *62*, 181–184. [[CrossRef](#)]
25. Assunção, A.; Martins, M.; Silva, G.; Lucas, H.; Coelho, M.R.; Costa, M.C. Bromate removal by anaerobic bacterial community: Mechanism and phylogenetic characterization. *J. Hazard. Mater.* **2011**, *197*, 237–243. [[CrossRef](#)] [[PubMed](#)]
26. Listiarini, K.; Tor, J.T.; Sun, D.D.; Leckie, J.O. Hybrid coagulation–nanofiltration membrane for removal of bromate and humic acid in water. *J. Membr. Sci.* **2010**, *365*, 154–159. [[CrossRef](#)]
27. Fischer, M.; Warneck, P. Photodecomposition and photooxidation of hydrogen sulfite in aqueous solution. *J. Phys. Chem. A* **1996**, *100*, 15111–15117. [[CrossRef](#)]
28. Lian, R.; Oulianov, D.A.; And, R.A.C.; Shkrob, I.A.; And, X.C.; Bradforth, S.E. Electron photodetachment from aqueous anions. 3. Dynamics of geminate pairs derived from photoexcitation of mono- vs polyatomic anions. *J. Phys. Chem. A* **2006**, *110*, 9071–9078. [[CrossRef](#)] [[PubMed](#)]
29. Ichino, T.; Fessenden, R.W. Reactions of hydrated electron with various radicals: Spin factor in diffusion-controlled reactions. *J. Phys. Chem. A* **2007**, *111*, 2527–2541. [[CrossRef](#)] [[PubMed](#)]
30. Sauer, M.C., Jr.; Crowell, R.A.; Shkrob, I.A. Electron photodetachment from aqueous anions. 1. Quantum yields for generation of hydrated electron by 193 and 248 nm laser photoexcitation of miscellaneous inorganic anions. *J. Phys. Chem. A* **2004**, *108*, 5490–5502. [[CrossRef](#)]
31. Alfassi, Z.B.; Huie, R.E.; Marguet, S.; Natarajan, E.; Neta, P. Rate constants for reactions of iodine atoms in solution. *Int. J. Chem. Kinet.* **1995**, *27*, 181–188. [[CrossRef](#)]
32. Jortner, J.; Levine, R.; Ottolenghi, M.; Stein, G. The photochemistry of the iodide ion in aqueous solution. *J. Phys. Chem.* **1961**, *65*, 1232–1238. [[CrossRef](#)]
33. Park, H.; Vecitis, C.D.; Cheng, J.; Dalleska, N.F.; Mader, B.T.; Hoffmann, M.R. Reductive degradation of perfluoroalkyl compounds with aquated electrons generated from iodide photolysis at 254 nm. *Photochem. Photobiol. Sci.* **2011**, *10*, 1945–1953. [[CrossRef](#)] [[PubMed](#)]
34. Neta, P.; Huie, R.E.; Ross, A.B. Rate constants for reactions of inorganic radicals in aqueous solution. *J. Phys. Chem. Ref. Data* **1988**, *17*, 1027–1284. [[CrossRef](#)]
35. Yiin, B.S.; Margerum, D.W. Nonmetal redox kinetics: Reactions of iodine and triiodide with sulfite and hydrogen sulfite and the hydrolysis of iodosulfate. *Inorg. Chem.* **1990**, *29*, 1559–1564. [[CrossRef](#)]
36. Hayon, E.; Treinin, A.; Wilf, J. Electronic spectra, photochemistry, and autoxidation mechanism of the sulfite-bisulfite-pyrosulfite systems SO_2^- , SO_3^- , SO_4^- , and SO_5^- radicals. *J. Am. Chem. Soc.* **1972**, *94*, 47–57. [[CrossRef](#)]
37. Grebel, J.E.; Pignatello, J.J.; Mitch, W.A. Effect of halide ions and carbonates on organic contaminant degradation by hydroxyl radical-based advanced oxidation processes in saline waters. *Environ. Sci. Technol.* **2010**, *44*, 6822–6828. [[CrossRef](#)]
38. Ross, A.B.; Neta, P. *Rate Constants for Reactions of Inorganic Radicals in Aqueous-Solution*; Report NSRDS-NBS65; National Bureau of Standards: Washington, DC, USA, 1979; pp. 5–6.
39. Neta, P.; Huie, R.E. Free-radical chemistry of sulfite. *Environ. Health Perspect.* **1985**, *64*, 209–217. [[CrossRef](#)]
40. Buchanan, W.; Roddick, F.; Porter, N.; Drikass, M. Fractionation of UV and VUV pretreated natural organic matter from drinking water. *Environ. Sci. Technol.* **2005**, *39*, 4647–4654. [[CrossRef](#)]
41. Kishore, K.; Moorthy, P.N.; Rao, K.N. Use of riboflavin as a standard solute for estimating H-atom reaction rate constants by competition kinetic method. *Radiat. Phys. Chem.* **1984**, *23*, 495–497. [[CrossRef](#)]
42. Zelinsky, A.G.; Pirogov, B.Y. Electrochemical oxidation of sulfite and sulfur dioxide at a renewable graphite electrode. *Electrochim. Acta* **2017**, *231*, 371–378. [[CrossRef](#)]
43. Xiao, Q.; Ren, Y.; Yu, S. Pilot study on bromate reduction from drinking water by UV/sulfite systems: Economic cost comparisons, effects of environmental parameters and mechanisms. *Chem. Eng. J.* **2017**, *330*, 1203–1210. [[CrossRef](#)]
44. Wenk, J.; von Gunten, U.; Canonica, S. Effect of dissolved organic matter on the transformation of contaminants induced by excited triplet states and the hydroxyl radical. *Environ. Sci. Technol.* **2011**, *45*, 1334–1340. [[CrossRef](#)] [[PubMed](#)]

45. Ji, Y.; Zhou, L.; Ferronato, C.; Yang, X.; Salvador, A.; Zeng, C.; Chovelon, J.M. Photocatalytic degradation of atenolol in aqueous titanium dioxide suspensions: Kinetics, intermediates and degradation pathways. *J. Photochem. Photobiol. A Chem.* **2013**, *254*, 35–44. [[CrossRef](#)]
46. Fang, J.; Shang, C. Bromate formation from bromide oxidation by the UV/persulfate process. *Environ. Sci. Technol.* **2012**, *46*, 8976–8983. [[CrossRef](#)] [[PubMed](#)]
47. Liu, L.; Li, W.; Zheng, B.; Mao, S.; Jin, H. Comparative study on the determination of bicarbonate in bicarbonated ringer s injection by titrimetric method and suppressed ion chromatography. *West China J. Pharm. Sci.* **2016**, *31*, 286–288. [[CrossRef](#)]
48. Rosenfeldt, E.J.; Linden, K.G.; Canonica, S.; Gunten, U.V. Comparison of the efficiency of ·OH radical formation during ozonation and the advanced oxidation processes O₃/H₂O₂ and UV/H₂O₂. *Water Res.* **2006**, *40*, 3695–3704. [[CrossRef](#)] [[PubMed](#)]



© 2018 by the authors. Licensee MDPI, Basel, Switzerland. This article is an open access article distributed under the terms and conditions of the Creative Commons Attribution (CC BY) license (<http://creativecommons.org/licenses/by/4.0/>).